ELSEVIER

Biophysical Chemistry 111 (2004) 35–42

Biophysical Chemistry

www.elsevier.com/locate/bpc

Low frequency ultrasound induces aggregation of porcine fumarase by free radicals production

M. Barteri[a,*], M. Diociaiuti[b], A. Pala[c], S. Rotella[a]

[a] *Dipartimento di Chimica, Università degli Studi di Roma "La Sapienza", Piazzale A. Moro 5-00185 Rome, Italy*
[b] *Istituto Superiore di Sanità, Laboratorio di Ultrastrutture, Viale Regina Elena 299-00161 Rome, Italy*
[c] *Laboratorio di Biochimica degli Ormoni Sessuali, Clinica Ostetrica e Ginecologica, Università degli Studi di Roma "La Sapienza", Piazzale A. Moro 5-00185 Rome, Italy*

Received 7 April 2004; accepted 12 April 2004
Available online 6 May 2004

Abstract

Hydrogen peroxide and hydroxyl-free radicals determine a diffuse aggregation of porcine fumarase and a loss of its enzymatic activity. In this study, hydroxyl-free radicals were generated "in situ" by irradiation with ultrasound (US) at 38 kHz. The structural characteristics of aggregated fumarase were studied using circular dichroism spectroscopy (CD) and steady state fluorescence spectroscopy. Enzyme aggregation is caused by the formation of intermolecular disufide bridges, originated by the oxidation of cysteine residues, together with a diffuse increase in β-turn in the protein's secondary structure. These conformational changes lead to a fibrous, amyloid-like aggregation which appears ordered and regular under TEM microscopy.

Keywords: Free radicals; Hydrogen peroxide; Fumarase; Amyloid-like aggregation

1. Introduction

A large number of studies [1–6] on the role of oxidative stress in human pathologies emphasize the importance of enzymatic and non-enzymatic sources capable of overproduction of free radicals when provoked by alterations in electron transport mechanisms [7–9].Under normal conditions, "in vivo" accumulation of toxic peroxides and related free radicals is efficiently controlled by an array of antioxidant systems [10,11]. In particular, hydrogen peroxide and hydroxyl-free radicals are widely regarded as cytotoxic agents and considered responsible for chemical and structural modifications to DNA, lipid and proteins [12–14]. Overproduction of H_2O_2 in isolated mitochondria depends on their metabolic state, and is commonly based on non-enzymatic reactions. It is likely that this condition increases reduction of components of the electron-transfer chain (e.g. the presence of uncouples, mitochondrial inhibitors, O_2 concentration) and thus leads to a higher rate of H_2O_2 production and accumulation [15,16]. In aerobic organisms, molecular oxygen chemically oxidizes redox enzymes, forming superoxide ($O_2^{\cdot -}$), hydrogen peroxide and hydroxyl-free radicals. These organisms cannot efficiently scavenge endogenous H_2O_2 and free radicals and they grow poorly or die indicating that these species are formed in potentially toxic doses inside living cells.

Similar toxicity occurs in wild-type organisms when they are exposed to higher-than-usual levels of oxygen, evidently because these species are formed at elevated rates. Although this is an area of broad concern, "in vivo" measurement of highly reactive hydroxyl radicals is very difficult because neither the rate of oxidant production nor the steady state levels of reactive oxygen free radicals are easily measured in biological systems [17]. It has also been observed that modifications of the structural and conformational properties of mitochondrial and cytosolic forms of human fumarase cause severe neurological impairment [18] and that specific biochemical defects affecting the Krebs cycle revealed a marked fumarase deficiency [19]. This enzyme catalyzes the reversible stereospecific addition of water to

Abbreviations: US, ultrasound; CD, circular dichroism; TEM, Transmission Electron Microscopy; ME-2, mercaptoethanol; PDB, Protein Data Bank; PM, (*N*-(1-pyrenyl) maleimide).

* Corresponding author. Tel.: +39-6-49913957; fax: +39-6-490631.
E-mail address: mario.barteri@uniroma1.it (M. Barteri).

0301-4622/$ - see front matter © 2004 Elsevier B.V. All rights reserved.
doi:10.1016/j.bpc.2004.04.002

fumaric acid to give the (*S*)(−)L-malate. It has been found that any significant defect is incompatible with life [20–22], thus demonstrating the central role that it plays in the metabolism of living cells.

The main purpose of this experimental research was to show that hydrogen peroxide and hydroxyl-free radicals cause a diffuse protein aggregation and complete loss of fumarase enzymatic activity. The study was performed "in vitro". Porcine fumarase was used for its structural similarity and extensive sequence homology ($\geq 96\%$) with both mitochondrial and cytosolic human fumarases. In the porcine enzyme, quaternary structure consists of a tetramer of identical 50-kDa molecular mass subunits [23–25]. Although this protein was purified and crystallized for the first time in 1952 [26], the unit cell dimensions, space group and the number of molecules per cell from preliminary X-ray data were reported only in 1986 by Sacchettini et al. [27] and its crystallographic coordinates have not yet been reported.

We generated "in situ" hydroxyl-free radicals by irradiation of an aqueous solution with ultrasound (US) at 38 kHz since low frequency (<1 MHz) US irradiation yields effects and products similar to those observed with X-ray and γ-radiolysis. We also wished to avoid using Fenton's reagent, as the binding of heavy metal ions (e.g. the iron in Fenton's reagent) to protein which can induce conformational changes in the secondary and tertiary fumarase structure.

2. Materials and methods

Highly purified porcine fumarase was purchased from Sigma (St. Louis, MO, USA) as a suspension in 3.2 M $(NH_4)_2SO_4$, 0.05 M KH_2PO_4, 14 mM ME. Enzyme purity was checked by HPLC analysis using a Superdex 200 HR10/30 column (Amersham Pharmacia Biotech), and was found to correspond to that declared by Sigma. Protein concentration was determined spectrophotometrically at 280 nm (0.1 M PBS, pH = 7.3 ± 0.1) with $A_{280\ nm}^{1\ mg/ml} = 0.51$ [28]. CD spectra were recorded on a Jasco J-715 spectropolarimeter, equipped with a computer data processor and a temperature-controlled QS cuvette holder. Cuvettes of 1–10-mm path length were used. Fluorescence experiments were carried out in 0.1 M PBS buffer. For free cysteine quantification, 3.09 μM (0.6 mg/ml; MW = 194 kDa) solutions of native and irradiated porcine fumarase were placed in the cell of a Varian Eclipse spectrofluorimeter and mixed into the cell with 1 10^{-3} M (*N*-(1-pyrenyl) maleimide) (PM). Fluorescence intensity at 396 nm using excitation at 342 nm was measured at $T = 25.0 \pm 0.1$ °C. Fumaric acid hydration reaction kinetics were readily followed spectrophotometrically due to the absorption in the UV region (270–300 nm) of the fumaric acid double bond. Measurements were made in a quartz cuvette with 10-mm optical path placed at controlled temperature in a photodiode array spectrophotometer Hewlett-Packard 8452A.

Ultrasound irradiations were carried out in a 38-kHz UNISET-AC bath, equipped with temperature-controlled glassware allowing irradiation to be performed in an argon atmosphere. TEM images were collected by a Zeiss 902 TEM, operating at 80 kV. Negative protein staining was obtained with PTA (2% w/v solution of phosphotungstate acid) buffered at pH = 7.3; the attainable resolution was evaluated as in the order of 2 nm.

3. Results and discussion

Protein Data Bank (PDB) contains several fumarase crystal structures (yeast and *E. coli*) but, despite the strong similarity of amino acid sequences in this family, the main difference between these enzymes and the porcine protein is the number of free cysteine residues. Porcine fumarase has only three cysteines (Cys_{289}, Cys_{333} and Cys_{390}) and no disulfide bridges. As its crystallographic coordinates are not

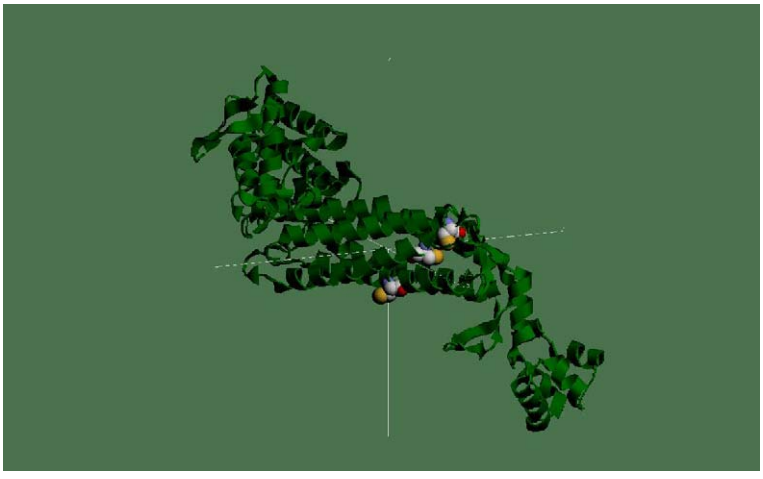

Fig. 1. Computer-aided simulation of porcine fumarase tertiary structure. Calculations were performed by Swiss-Prot set programs, comparing fumarase homology with 240 different proteins. The enzyme backbone is depicted as "ribbon" and cysteine residues are represented as "spacefill" model.

yet known, we calculated the tertiary structure of monomeric porcine fumarase using suitable computer programs [29–31] comparing its homologies with about 240 different protein structures.

Fig. 1 shows the structure we calculated, where the protein backbone is pictured as solid ribbon, and the atoms of cysteine residues are represented as spacefill model.

4. Aerobic protein aging

To prevent cysteine oxidation, fumarase from porcine heart was conserved as a suspension in aqueous solution containing 14 mM 2-mercaptoethanol (ME). In these conditions, the enzyme maintains its catalytic activity for several months if correctly stored ($T = 4$ °C). In general, enzyme solutions were prepared by diluting the aqueous fumarase suspension, however, at room temperature diluted solutions were not stable, and enzymatic activity gradually decreased. We carried out kinetic experiments ($T = 25.0 \pm 0.1$ °C) on the fumarate hydration reaction over several days, using the same protein stock solution previously dialyzed against PBS buffer (0.1 M, potassium phosphate pH 7.3) to remove ME. We found that after 24 h, enzymatic activity was reduced by about 15–20% and after 10 days, the activity was completely inhibited even though the enzyme stock solution had been stored in a dark bottle at 4 °C (data not shown).

The native fumarase solutions underwent slow and progressive inactivation, as the oxygen dissolved in the solution would have oxidized Cys residues. Fig. 2A shows that, over time, slow changes in CD spectra occur: straight after preparation, the fumarase solution exhibited a spectrum with double minima at 208 and 222 nm, demonstrating that the α-helix conformation is predominant in the native protein structure (curve a). The sample's secondary structure composition was evaluated from the best fit of the experimental CD measurement [32]. This yielded α-helix = 56.5%, β-sheet = 13.1%, β-turn = 7.9% and random = 22.5%, values very close to those found by Beekmans and Kanarek [33].

The same sample analyzed after 24 h and 10 days (curves b and c of Fig. 2A) showed a detectable protein precipitation. To eliminate the misleading contribution from light scattered by aggregates, aged samples were centrifuged before recording CD spectra. As expected, the decrease in soluble protein concentration led to a reduction in intensities at 195 nm (positive) and two (negative) bands at 208 and 222 nm. CD spectra in Fig. 2 are plotted as ellipticity θ (degree) vs. wavelength, to better demonstrate that oxidation causes a reduction of protein concentration. Molar ellipticities taking account of changes in protein concentration give highly reproducible [θ] vs. wavelength CD plots. These spectra did not show a significant variation in the secondary structure, as there was no change in minima and ratio positions of their intensities. However, enzyme solution prepared and conserved under argon atmosphere showed no precipitates and maintained unaltered CD intensities and catalytic activity, thus confirming the hypothesis that dissolved oxygen oxidizes cysteine residues, giving rise to the formation of disulfide intermolecular bonds.

5. Effect of hydrogen peroxide

Among the possible targets of cellular damage, oxidation of mitochondrial enzymes such as fumarase may be considered a relevant process [34]. However, a dramatic lack occur despite the paramount importance of fumarase activity. In the human body, H_2O_2 may be increased by superoxide radical ion ($O_2^{\cdot -}$) dismutation, which is influenced by diet, aging and/or pathologic alterations. Urinary H_2O_2 concentration has recently been proposed as a valuable biomarker of oxidative stress level [17]. However, insufficient information has been gathered on possible conforma-

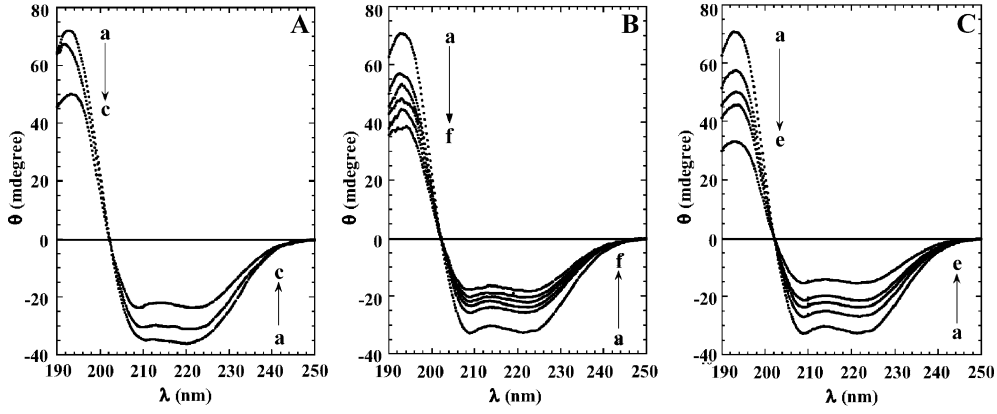

Fig. 2. CD spectra of native fumarase recorded immediately after preparation (curve a), after 24 h (curve b) and after 10 days (curve c) (panel A). CD spectra of wild-type fumarase (a) and fumarase with H_2O_2 concentrations of: 1.8×10^{-3} M (b); 3.6×10^{-3} M (c); 5.4×10^{-3} M (d); 9.0×10^{-3} M (e); 13.8×10^{-3} M (f) (panel B). In the panel C, CD spectra of native fumarase and after 5, 10, 20 and 30 min of US irradiation (curves a–e) are shown. In all spectra, intensities decrease as a consequence of aggregate precipitation.

tion changes induced by H_2O_2 on mitochondrial proteins and, in particular, on fumarase.

We prepared buffered solutions of native porcine fumarase (0.6 mg/ml) to which were added appropriate amounts of a concentrated stock solution of H_2O_2, to give final concentrations between 1.8 and 13.8 mM. These solutions were centrifuged after about 1 h of incubation ($T = 25.0 \pm 0.1$ °C) and their CD spectra recorded. Fig. 2B shows that in the presence of H_2O_2, the dichroic spectra intensities decreased, confirming that the oxidation reaction was responsible for fumarase aggregation.

Comparing these data with those obtained from observation of the slow protein aerobic oxidation process (aging), it is evident that H_2O_2 increases the rate of oxidation reaction and consequently the rate of enzyme aggregation (compare Fig. 2A vs. B).

6. Oxidative effect of ultrasound irradiation

In aqueous solution, low frequency (20 kHz $< \nu <$ 1000 kHz) US generates oxygen free radicals as a consequence of the physical phenomenon known as "cavitation". Sound is transmitted as a wave through alternating compression and rarefaction cycles. In the rarefaction stage, the ultrasound provokes the formation of a large number of gas (and/or solvent vapor) microbubbles. Successive compression brings about an instantaneous collapse of these microbubbles and the release of considerable amounts of energy. The "local" temperature and pressure of the bubbles can increase by thousands of degrees (K) and up to 10,000 atmospheres [35]. Under these extreme physical conditions, ultrasonic irradiation gives rise to homolytic water molecule cleavage, generating high energy intermediates such as hydroxyl and hydrogen free radicals, whose presence has been confirmed by electron-spin resonance spectroscopy using spin-trapping techniques [36–39].

$$H_2O \xrightarrow{US} H\cdot + HO\cdot$$

$$2H\cdot \rightarrow H_2$$

$$H\cdot + H_2O \rightarrow H_2 + HO\cdot$$

$$2HO\cdot \rightarrow H_2O_2$$

These oxidative species are responsible for the extensive degradation of proteins, nucleic acids, and polysaccharides. When assessing the extent of damage to a biological system caused by exposure to US, it is therefore important to monitor and quantify the radicals formed.

Hydroxyl-free radical concentration was determined by Fricke's method [40], a simple system to monitor free radical activity which requires very basic procedures. Fricke's reagent contains $FeSO_4$ (1 mM), H_2SO_4 (0.4 M) and NaCl (1 mM) and gives a linear dose–response relationship, allowing quantification of hydroxyl radicals (HO·) produced by sonication. Conversely, other calibration methods, such as those based on the oxidation of 7-(hydroxycumarine) or terephthalic acid [41], did not give a linear calibration curve in the HO· concentration range analyzed.

Fig. 2C shows CD spectra of the native fumarase solution and the same solution after US irradiation for 5, 10, 20 and 30 min. CD spectra were recorded immediately after centrifugation. The effect of free radicals produced by US irradiation is practically identical to that of free radicals produced by H_2O_2. It should be remembered that under irradiation, H_2O_2 is the major product of the HO· recombination reaction. However, in electron-transfer reactions between H_2O_2 and reductans, the presence of free radicals is well documented [5].

The progressive oxidation of cysteine residues under US was also analyzed, by steady state fluorescence measurements of fumarase solution in the presence of PM. This reagent, proposed as an alternative to Ellman's reagent (5,5′-dithiobis (2-nitrobenzoic acid)) [42], was used to titrate the protein's free thiol groups.

In aqueous solution, maleimide is a non-fluorescent compound but it forms strongly fluorescent adducts with thiol groups. The mechanism proposed for this reaction supposes the rapid addition of the cysteine SH group to the olefinic double bond in the PM maleimide moiety, to form *S*-[*N*-(1-pyrene) succinoimido]cysteine which rapidly rearranges into a fluorescent thiazane derivative [43].

The excitation wavelength of the pyrene chromophore was 342 nm and the fluorescence emission spectra of the labeled fumarase were recorded after 15 min of incubation at 37 °C. Identical aliquots (1 ml) of the same native protein solution were irradiated by increasing the sonication time; spectra were recorded at controlled temperature under the same experimental conditions. Fig. 3 shows that the fluorescence to adduct intensity between PM and native protein cysteines progressively decreases after 3, 5, 6, 8, 10, 13 and 20 min of US irradiation.

The decrease in fluorescence intensity is proportional to residual-free cysteine sulfide group concentration, confirming that enzyme inactivation is due to the formation of disulfide-linked aggregates. Although progressive oxidation of the -SH cysteine group to cysteic acid or to mixed disulfide cannot be excluded, we found a negligible consecutive oxidation reaction under our experimental conditions.

Hydroxyl-free radicals can also oxidize the side-chains of amino acid residues, such as Phe, Tyr, Trp, and His, thus inducing modification of the protein primary structure [35]. Some stable oxidation products such as aspartate, produced on oxidation of histidine, and o-tyrosine and *m*-tyrosine, formed by phenylalanine hydroxylation, are indistinguishable forms of the natural amino acid in protein. In this case, the loss in free stabilization energy of the wild-type proteins may be considered similar to that observed as a consequence of mutation [36]. In the near UV region (250–350

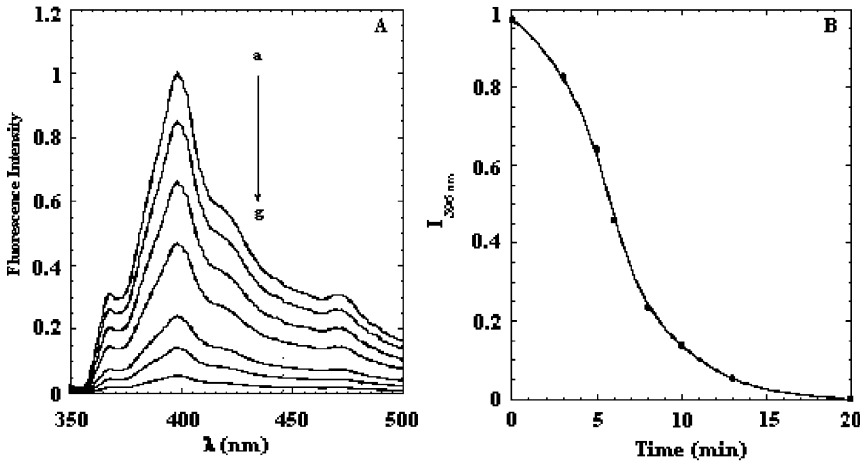

Fig. 3. (A) Fluorescence emission spectra of the adduct between PM and cysteines of the residual soluble protein after 0, 3, 5, 6, 8, 10 and 13 min of US irradiation (curves a–g). After 20 min, fluorescence intensity was zero. Fumarase was 0.6 mg/ml, PBS 0.1 M, pH 7.3 ± 0.1. Emission spectra (bandwidth 10 nm) of the labeled fumarase were recorded after 15 min of incubation with PM at $T = 37$ °C. Excitation wavelength (bandwidth 3 nm) was 342 nm. (B) Decrease of relative fluorescence intensity at 396 nm vs. US irradiation time.

nm), CD is sensitive to the optically active absorption of aromatic residues (e.g. Tyr, Tpr, and Phe), as well as to conformational changes of the tertiary structure. Within experimental error, all our samples yielded identical molar ellipticities [θ] values (data not shown). This can be considered as indirect evidence that Tyr, Trp and Phe residues of our protein samples do not react with H_2O_2 or US-produced free radicals.

7. Structural investigation by TEM

The main consequence of aggregation is a rapid decrease in protein solubility, producing a detectable fumarase precipitate. This was collected and studied by TEM [44,45]. This technique has the advantage of giving high resolution pictures of the specimen, thus enabling valuable information to be obtained on protein aggregate features.

Fig. 4 shows TEM micrographs for both native and US-irradiated fumarase. The heavy metal (W) salts used for TEM sample preparation give good radiation protection and thus maintain specimen integrity. In addition, heavy metal around the protein itself scatters electrons more efficiently than the molecule alone, giving greater image contrast and allowing detailed examination of the structure.

Fig. 4A (left) depicts the native protein sample and clearly shows isolated, quasi-circular white spots of about 5 nm, corresponding to the tetrameric form of the native protein molecules. Fig. 4B (right) shows fumarase at the same magnification, after 30-min US irradiation. The aggregates appear as well-defined fibers with a very regular rod-

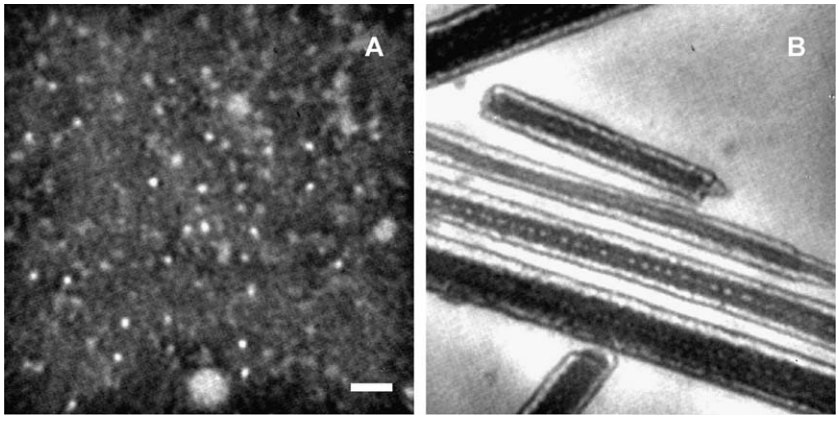

Fig. 4. TEM images of fumarase samples stained with PTA (2% w/v solution of phosphotungstate acid) buffered at pH 7.3. Micrographs A (native) and B (sonicated 30 min) were obtained by splitting a solution of native porcine fumarase in two aliquots. Sample B was irradiated immediately and after negative staining, both A and B samples were analyzed. To enhance contrast, the microscope was settled with Electron Energy Loss imaging filter, which allows collection of elastic electrons only ($\Delta E = 0$), thus avoiding the contribution of inelastic electrons to contrast formation. Inelastic electrons scattered from the sample contribute only to image background noise and filtering them out strongly enhances final image quality. The attainable resolution was evaluated as in the order of 2 nm. The white bar corresponds to 40 nm.

like shape of variable size and thickness, all characterized by an internal structure made of quasi-circular subunits. They are very similar to those in Fig. 4A but are ordered in arrays oriented towards the main fiber axis. The border arrays have better contrast than the inner arrays, probably due to an irregular distribution of the staining metal inside the protein arrangement. The distance between two adjacent arrays is around 12 nm. However, a distance of 6 nm can be measured where the distribution of the staining metal allows resolution of intermediate arrays.

The TEM image in Fig. 4B also reveals that the inner structures of the rod-like aggregates have regular features, probably generated by the ordered binding of fumarase molecules.

8. CD study of fumarase fibrils

In aqueous solution, fumarase has a circular dichroism (CD) spectrum indicating an ordered secondary structure rich in the α-helix fraction. Changes in the secondary fumarase structure of the aggregated enzyme can be excluded. To obtain the spectrum of fumarase fibrils, we adopted the experimental procedure suggested by Arvinte [47]: a small piece of aggregate was pressed between the silica plates of a 0.1-mm CD cuvette. In this narrow path, homogeneous distribution of materials suitable for correct CD measurement was obtained. A comparison between native and sonicated spectra is shown in Fig. 5.

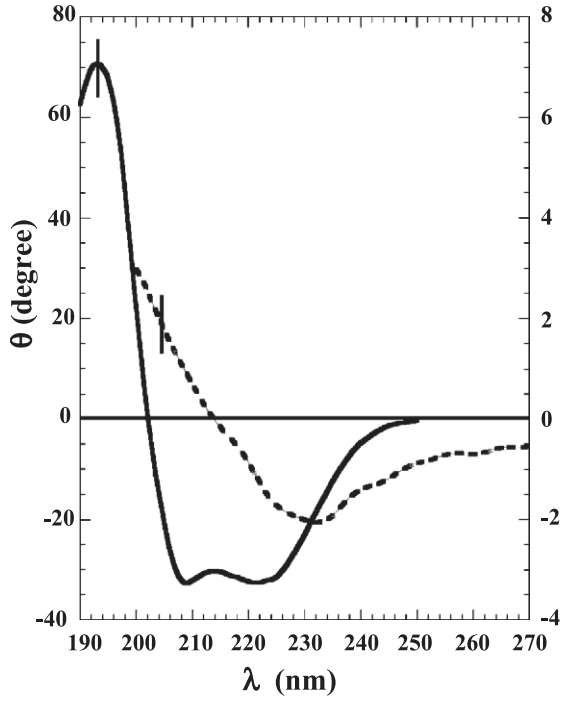

Fig. 5. Comparison between CD spectra of native (full line) and aggregated (dotted line) fumarase. The spectrum of fumarase fibrils was obtained with the procedure reported in Ref. [45].

As already described, native protein exhibited two well-defined minima at 208 and 222 nm due to the presence of a high (56–58%) α-helix content and about 20% beta structure in the secondary structure. After oxidation, the aggregated protein secondary structure was greatly modified, with a shoulder at 218 nm and a deeper minimum at 232 nm, evidently due to an increase in β-turn. CD spectra of antiparallel β-sheet showed a deep minimum at 217 nm, while the β-turn structure was characterized by a large absorption between 225 and 235 nm. The aggregate spectrum showed both these characteristics, as well as a diffuse negative absorption between 250 and 260 nm attributed to an asymmetric disulfide group in gauche conformation [46]. This experimental evidence indicates that at least two different conformational changes concurred to generate a thermodynamically stable aggregate. The formation of a large network of disulfide bridges forces the protein structure to assume and propagate the content of β conformation, thus increasing intermolecular hydrophobic interactions with a mechanism reminiscent of that already suggested for β-amyloid aggregation.

9. Conclusions

Low frequency US is widely used for extraction of biological materials such as proteins, hormones, lipids and nucleic acids. However, it is known that US irradiation is a powerful source of "in situ" hydroxyl-free radicals production. Due to this concern, we have undertaken the study on the US effect on fumarase structural and catalytic properties directing our in vitro experimental work to porcine fumarase molecules because of its high homology to human fumarase. In a living cell, when the redox equilibria go out of control, a disulfide bridge network is formed which leads to a protein–protein aggregation. Such aggregation is widely recognized cause of pathological status in humans and animals. In addition being this kind of aggregation a common feature of many proteins, the phenomenon is of general interest and involves different tissues and organs. Furthermore, the free radicals overproduction has been documented as an important physiological alteration that origins protein aggregation and amyloidosis.

In these studies, we showed that the enzyme aggregation is caused by hydrogen peroxide and/or HO-free radicals which are responsible for a complex aggregation mechanism, driven by intermolecular disulfide bonds and stabilized by amyloid-like hydrophobic interactions. We found that cysteine residues are particularly sensitive to oxidation by free radicals and, even under mild conditions, they are converted to disulfide by preferential oxidation. In biological systems, disulfide reductase can convert oxidized forms of cysteine back to their unmodified forms, however, amyloid-like aggregation may forbid this conversion. This fact is matter of our further in vitro investigation.

Acknowledgements

This study was financed by MURST. Authors are particularly grateful to Prof. P. De Santis for his helpful advice.

References

[1] O. Aruoma, B. Halliwell, Molecular Biology of Free Radicals in Human Disease, Saint Lucia OICA International, USA, 1998.
[2] J.W. Baynes, Role of oxidative stress in development of complications in diabetes, Diabetes 40 (1991) 405–412.
[3] L. Flohè, R. Beckman, Oxygen centered free radicals as mediators of inflammation, in: H. Sies, H. Giertz, G. Loschen, H. Sies (Eds.), Oxidative stress, New York Academic Press, 1985, pp. 403–435.
[4] B. Halliwell, J.M.C. Gutteridge, in: B. Halliwell, J.M.C. Gutteridge (Eds.), Free radicals in Biology and Medicine, 2nd ed., Claredon Press, Oxford, 1989, pp. 416–508.
[5] B. Halliwell, J.M.C. Gutteridge, in: B. Halliwell, J.M.C. Gutteridge (Eds.), Free radicals in biology and medicine, Claredon Press, Oxford, 1989, pp. 22–85.
[6] L.W. Oberly, Free radicals and diabetes, Free Radic. Biol. Med. 5 (1988) 113–124.
[7] E. Fujimori, Cross-linking and fluorescence changes of collagen by glycation and oxidation, Biochim. Biophys. Acta 99 (1989) 105–110.
[8] S.P. Kantrow, L.G. Tatro, C.A. Piantadosi, Oxidative stress and adenine nucleotide control of mitochondrial permeability transition, Free Radic. Biol. Med. 28 (2000) 251–260.
[9] L.P. Liang, Y.S. Ho, M. Patel, Mitochondrial superoxide production in kainate-induced hippocampal damage, Neuroscience 101 (2000) 563–570.
[10] V.W. Bowry, K.U. Ingold, The unexpected role of vitamin E (α-tocopherol) in the peroxidation of human low-density lipoproteins, Acc. Chem. Res. 32 (1999) 27–34.
[11] C. Rice-Evans, A. Diplock, Current status of antioxidant therapy, Free Radic. Biol. Med. 15 (2000) 77–96.
[12] J.V. Hunt, C.C.T. Smith, S.P. Wolff, Autoxidative glycosylation and possible involvement of peroxides and free radical in LDL modification by glucose, Diabetes 39 (1990) 1420–1424.
[13] K. Keyer, J.A. Imlay, Superoxide accelerates DNA damage by elevating free-iron levels, Proc. Natl. Acad. Sci. U. S. A. 93 (1996) 13635–13640.
[14] J.A. Imlay, Toxic DNA damage by hydrogen peroxide through the Fenton reaction in vivo and in vitro, Linn S. Sci. 240 (1988) 640–642.
[15] C. Giulivi, A. Boveris, E. Cadenas, Hydroxyl radical generation during mitochondrial electron-transfer and formation of 8-hydroxydesoxy-guanosine in mitochondrial DNA, Arch. Biochem. Biophys. 316 (1995) 909–916.
[16] B. Halliwell, M. Grootveld, J.M.C. Gutteridge, Methods for the measurement of hydroxyl radical in biochemical systems: deoxyribose degradation and aromatic hydroxylation, in: D. Glick (Ed.), Methods of Biochemical Analysis, vol. 33, Wiley, New York, 1987, pp. 59–90.
[17] B. Halliwell, M.V. Clement, L.H. Long, Hydrogen peroxide in the human body, FEBS Lett. 486 (2000) 10–13.
[18] D.T. Whelan, R.E. Hill, S. McClorry, Fumaric aciduria: a new organic aciduria, associated with mental retardation and speech impairment, Clin. Chim. Acta 132 (1983) 301–308.
[19] C. Gellera, G. Uziel, M. Rimoldi, M. Zeviani, A. Laverda, F. Carrara, S. Di Donato, Fumarase deficiency is an autosomal recessive encephalopathy affecting both the mitochondrial and cytosolic enzymes, Neurology 40 (1990) 495–499.
[20] A.B. Zinn, D.S. Kerr, C.L. Hoppel, Fumarase deficiency: a new cause of mitochondrial encephalomyopathy, N. Engl. J. Med. 315 (1986) 469–475.
[21] R.L. Hill, J.W. Teipel, in: P.D. Boyer (Ed.), The Enzymes, Academic Press, New York, 1971, pp. 539–571.
[22] P. Rustin, T. Bourgeron, B. Parfait, D. Chretien, A. Munnich, A. Rütig, Inborn errors of the Krebs cycle: a group of unusual mitochondrial disease in human, Biochim. Biophys. Acta 1361 (1997) 185–197.
[23] S. Beekmans, L. Kanarek, Subunit interactions in pig heart fumarase: I. Study of tetramer-dimer equilibrium in dilute urea solutions, Int. J. Biochem. 14 (11) (1982) 965–970.
[24] S. Beekmans, L. Kanarek, Subunit interactions in pig heart fumarase: II. Study of tetramer-dimer equilibrium in function of enzyme concentration and temperature, Int. J. Biochem. 14 (11) (1982) 971–975.
[25] S. Beekmans, L. Kanarek, Chicken heart fumarase: its purification and physical–chemical characterization. A comparison with the enzyme from pig heart, Int. J. Biochem. 14 (6) (1982) 453–460.
[26] V. Massey, The crystallization of fumarase, Biochem. J. 51 (1952) 484–490.
[27] J.C. Sacchettini, M.W. Frazier, D.C. Chiara, L.J. Banazak, G.A. Grant, Purification, crystallization and preliminary X-ray data for porcine fumarase, J. Biol. Chem. 261 (32) (1986) 15183–15185.
[28] S. Beekmans, L. Kanarek, A new purification procedure for fumarase based of affinity chromatography. Isolation and characterization of pig-liver fumarase, Eur. J. Biochem. 78 (1977) 437–444.
[29] Zs. Dosztànyi, A. Fiser, I. Simon, Stabilization centers in proteins: identification characterization and prediction, J. Mol. Biol. 272 (1997) 597–612.
[30] J. Garnier, J.F. Gibrat, B. Robson, Methods Enzymol. 266 (1996) 540–553.
[31] A. Bairoch, P. Bucher, K. Hofmann, The Proposite database, its status, Nucleic Acids Res. 25 (1997) 217–221.
[32] W.C. Johnson, Protein secondary structure and circular dichroism: a practical guide, Proteins 7 (1990) 205–214.
[33] S. Beeckmans, L. Kanarek, Structure and activity of swine heart fumarase in dilute urea solutions, Arch. Int. Physiol. Biochim. 81 (5) (1973) 956.
[34] A. Boveris, E. Cadenas, Production of superoxide radicals and hydrogen peroxide in mitochondria, in: L.W. Oberley (Ed.), Superoxide Dismutase, CRC Press, Boca Raton, 1982, pp. 15–30.
[35] K.S. Suslick, in: K.S. Suslick (Ed.), Ultrasound. Its Chemical, Physical and Biological Effects, VCH, USA, 1988, pp. 140–152.
[36] K. Makino, P. Riesz, E.S.R. of spin-trapped radicals in gamma-irradiated polycrystalline amino acids. Chromatographic separation of radicals, J. Am. Chem. Soc. 104 (1982) 3537–3539.
[37] K. Makino, M.M. Mossoba, P. Riesz, Formation of $OH^{\cdot}$ and $H^{\cdot}$, Radiat. Res. 96 (1983) 416–421.
[38] A.K. Jana, S. Agarwal, S.N. Chatterjee, Membrane lipid peroxidation by ultrasound: mechanism and implications, Radiat. Environ. Biophys. 25 (1986) 309–314.
[39] A.K. Jana, S. Agarwal, S.N. Chatterjee, The induction of lipid peroxidation in liposomal membrane by ultrasound and the role of hydroxyl radicals, Radiat. Res. 124 (1990) 7–14.
[40] G.J. Price, E.J. Lenz, The use of dosimeters to measure radical production in aqueous sonochemical systems, Ultrasonics 31 (6) (1993) 451–456.
[41] M.J. Chaichi, A.R. Karami, A. Shockravi, M. Shamsipur, Chemiluminescence characteristics of cumarin derivatives as blue fluorescers in peroxyoxalate-hydrogen peroxide system, Spectrochim. Acta, Part A: Mol. Biomol. Spectrosc. 59A (6) (2003) 1145–1150.
[42] J. Woodward, J. Tate, P.C. Herrnann, B.R.J. Evans, Comparison of Ellman's reagent with *N*-(1-pyrenyl)maleimide for the determination of free sulfhydryl groups in reduced cellobiohydrolase I from richoderma reesei, Biochem. Biophys. Methods 26 (1993) 121–129.
[43] C.W. Wu, L.R. Yarbrough, Y.-H.F. Wu, *N*-(1-pyrenyl)maleimide: a fluorescent cross-linking reagent, Biochemistry 15 (13) (1976) 2863–2868.

[44] R.F. Egerton, in: R.F. Egerton (Ed.), Electron energy loss spectroscopy, Plenum, New York, 1986, pp. 85–89.
[45] R.C. Valentine, B.M. Shapiro, E.R. Stadtman, Regulation of glutamine synthetase: XII. Electron microscopy of enzyme from *Escherichia coli*, Biochemistry 7 (1968) 2143–2152.
[46] T. Arvinte, A. Cudd, A.F. Drake, The structure and mechanism of formation of human calcitonin fibrils, J. Biol. Chem. 268 (9) (1993) 6415–6422.
[47] T. Arvinte, A.F. Drake, Comparative study of human and salmon calcitonin secondary structure in solutions with low dielectric constants, J. Biol. Chem. 268 (9) (1993) 6408–6414.